ACS APPLIED MATERIALS & INTERFACES

Research Article

www.acsami.org

Highly Stretchable Thermoset Fibers and Nonwovens Using Thiol−ene Photopolymerization

Kadhiravan Shanmuganathan,[†] Steven M. Elliot,[†] Austin P. Lane,[†] and Christopher J. Ellison*[,†,‡]

[†]McKetta Department of Chemical Engineering and [‡]Texas Materials Institute, The University of Texas at Austin, 200 East Dean Keeton Street Stop C0400, Austin, Texas 78712, United States

ABSTRACT: In this report, we describe the preparation and characterization of a new class of thermoset fibers with high elongation and elastic recovery. Integrating UV-activated thiol−ene photopolymerization and electrospinning, we demonstrate an environmentally friendly single step approach to convert small monomeric precursor molecules into highly elastic fibers and nonwoven mats. The fibers were derived by in situ photopolymerization of a trifunctional vinyl ether monomer and a tetrafunctional thiol. Although thermosets often offer good chemical and thermal stability, these fibers also have a high average elongation at break of 62%. The elastomeric nature of these vinyl-ether based fibers can be partly attributed to their subambient T_g and partly to the cross-link density, monomer structure, and resulting network homogeneity. Nonwoven mats of these fibers were also stretchable and exhibited a much higher elongation at break of about 85%. These thermoset stretchable fibers could have potential applications as textile, biomedical, hot chemical filtration, and composite materials.

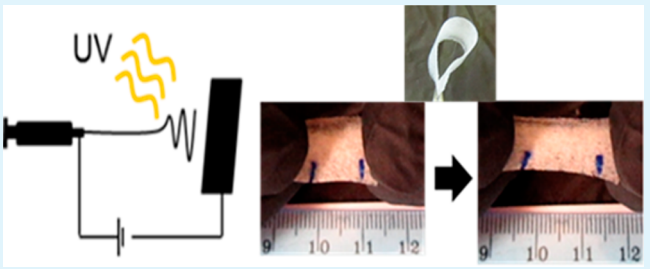

KEYWORDS: *elastomers, electrospinning, fiber, thiol−ene, photopolymerization, thermoset*

INTRODUCTION

Fibers with high elongation and good elastic recovery (elastomeric fibers) have been of interest for a number of applications such as apparel,[1] biological tissue scaffolds,[2] and shape-memory materials.[3] It is interesting to note that elastic fibers can be readily found in nature[4] in the orb webs of spiders, for example. The fibers that form the main structural elements of these webs has evolved as one of the toughest biological materials ever discovered, showing high strength and elongation with good elastic recovery.[5] In the past few years, scientists have made several attempts to replicate this material by genetically modifying diverse species such as plants,[6] bacteria,[7] and even animals,[8] to produce silk proteins that could later be reconstituted into fiber form. Though these attempts have given a better understanding of the structure and properties of these natural fibers, challenges still exist in understanding the complicated biosynthesis and mimicking the unique mechanical behavior of spider silk and other natural silk fibers. Ever since rubber thread found use in textiles,[9] several synthetic elastomeric fibers have been introduced such as nylon (polyamide), the first synthetic fiber, and "Spandex" (segmented polyurethane). In fact DuPont, the company that developed nylon, cites spider silk as a key inspiration for the material.[10]

Elasticity in nylon and Spandex arises from the entropic preference of polymer chains to exist in a coiled state.[11] When the fiber is stretched, the polymer chains uncoil into an entropically unfavorable state, and when it is released, they revert to their original coiled form. In addition, these polymers have crystalline domains that bind many chains together in a physical cross-link and prevent the chains from flowing past each other. In such semicrystalline linear thermoplastic polymers, their elastomeric mechanical behavior is limited to moderate temperatures (i.e., below their melt transition temperature). New methods of producing chemically cross-linked elastomeric fibers have been introduced in the past few years. These include the use of a carrier polymer to stabilize a photo-cross-linkable prepolymer mixture in a fiber,[2] the electrospinning of core/shell fiber structures followed by postspinning vulcanization of the core,[12] and simultaneous UV curing and electrospinning of preformed oligomers.[13] All of the above approaches to make elastomeric fibers require solvent or heat to prepare, and most cross-linking methods require an additional post-production step to make a covalently bonded network. In this report, we demonstrate an environmentally friendly single step approach to convert small monomeric precursor molecules into highly elastic thermoset fibers and nonwoven mats.

One of the most fascinating aspects of spider silk is the spider's ability to form fibers at ambient conditions, without using heat or toxic solvents. Inspired by this natural model, we recently demonstrated a greener fiber manufacturing approach combining UV-activated thiol−ene photopolymerization and the electrospinning process, wherein a mixture of non-volatile

Received: June 6, 2014
Accepted: July 30, 2014
Published: July 30, 2014

Scheme 1. Chemical Structures of Tetrafunctional Thiol, Pentafunctional Acrylate, Trifunctional Vinyl Ether, and Photoinitiator: (a) tris(4-(vinyloxy) butyl) trimellitate (TVE), (b) pentaerythritol tetrakis(3-mercaptopropionate) (PETT), (c) phenyl bis(2,4,6-tremethylbenzoyl)-phosphine oxide (Irgacure 2100), and (d) dipentaerythritol pentaacrylate (DPPA)

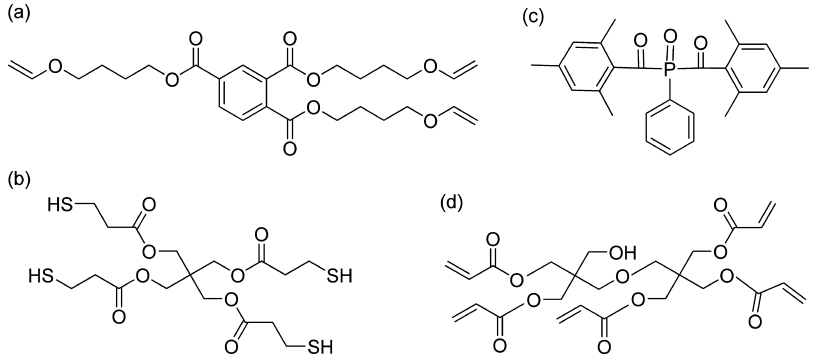

Scheme 2. Synthesis Scheme for TVE Monomer: (1) 1,2,4-tricarboxylic acid, (2) tetramethylene glycol monovinyl ether, (3) tris(4-(vinyloxy) butyl) trimellitate

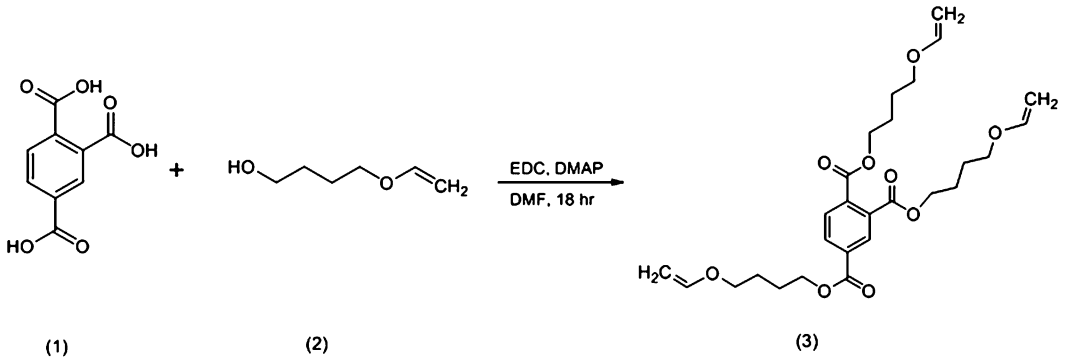

monomers were converted into fibers without using any solvent or heat.[14] In our proof of concept work,[14] the fibers were made from a pentafunctional acrylate and tetrafunctional thiol and had a moderate elongation at break of only 8−13%. Given the versatility of thiol−ene chemistry, we were motivated to tune the mechanical properties of the thiol−ene fibers using different monomer structures and functionalities. In a typical thiol−ene photopolymerization, activated thiol groups react with vinyl functional groups creating a carbon-centered radical. Subsequent transfer of hydrogen between a thiol and this radical regenerates the thiyl radical.[15−18] Thus, alternating propagation/chain transfer reactions between thiols and vinyl functional groups forms the basis of step-growth thiol−ene polymerizations encountered in many vinyl monomers such as norbornenes, vinyl ethers and allyl ethers that do not readily homopolymerize.[19] However, certain vinyl containing monomers such as acrylates and methacrylates that can homopolymerize undergo a combination of chain and step-growth polymerizations.[19] Unlike traditional chain growth vinyl polymerizations, thiol−ene photopolymerizations are not inhibited by oxygen and can be conducted under ambient conditions.[20] In this work, we were primarily interested in using multifunctional vinyl ether monomers. Faster curing kinetics and better network homogeneity rendered by vinyl ethers as compared to (meth)acrylates, led us to anticipate a stronger influence on the mechanical properties of resultant fibers. This report demonstrates our successful approach to make fibers and nonwoven mats from a tetrafunctional thiol and trifunctional vinyl ether, with significant elongation (60−80%) and high elastic recovery.

EXPERIMENTAL SECTION

Materials. Pentaerythritol tetrakis (3-mercaptopropionate) (PETT) (boiling point: 519.9 °C at 760 mmHg) with a functionality of $f = 4$ and tris(4-(vinyloxy) butyl) trimellitate (Trivinyl ether, TVE) (boiling point: 597.7 °C at 760 mmHg) with functionality $f = 3$ were purchased from Sigma-Aldrich. TVE can also be easily synthesized in the laboratory (details are given in the following paragraph). Irgacure 2100 (based on phenylbis(2, 4, 6-trimethylbenzoyl)-phosphine oxide) was provided by BASF, Switzerland, and used as a photoinitiator. Poly(methyl methacrylate), PMMA (M_w = 1,500,000 g/mol M_w/M_n = 1.05) was purchased from Scientific Polymer Products. All chemicals were used as received. Scheme 1 shows the chemical structures of the *thiol* and *-vinyl* monomers and photoinitiator used in this work.

TVE was synthesized in the laboratory as outlined in Scheme 2. In a typical reaction, 1,2,4-tricarboxylic acid (5.23 g, 24.9 mmol) (**1**), tetramethylene glycol monovinyl ether (9.55 g, 82.2 mmol) (**2**), and 4-dimethylaminopyridine (0.912 g, 7.47 mmol) (DMAP) were mixed with 100 mL of DMF in a 250 mL round-bottomed flask equipped with a mechanical stirrer. 1-Ethyl-3-(3-(dimethylamino)propyl)-carbodiimide (15.76 g, 82.2 mmol) (EDC) was then added to the flask in large portions at room temperature. The reaction was stirred for 18 h, and the resulting suspension was filtered to remove unreacted EDC. The product solution was then concentrated in vacuo and subsequently dissolved in 200 mL of ethyl acetate. The resulting solution was washed successively with water (2 × 80 mL), aqueous $CuSO_4$ (2 × 50 mL), sat. $NaHCO_3$ (80 mL), and brine (80 mL). The organic layer was dried with $MgSO_4$ and concentrated. The crude product was purified by column chromatography (3:7 ethyl acetate:hexanes) to yield TVE (**3**) as a slightly yellow oil (3.52 g, 28% yield). The lower overall yield could be attributed to the lower yield of the EDC coupling reaction. Longer reaction times and/or higher concentrations of EDC could help to increase the yield. ^{1}H NMR ($CDCl_3$): δ 8.37 (s, 1H), 8.18 (d, 1H), 7.74 (d, 1H), 6.45 (m,

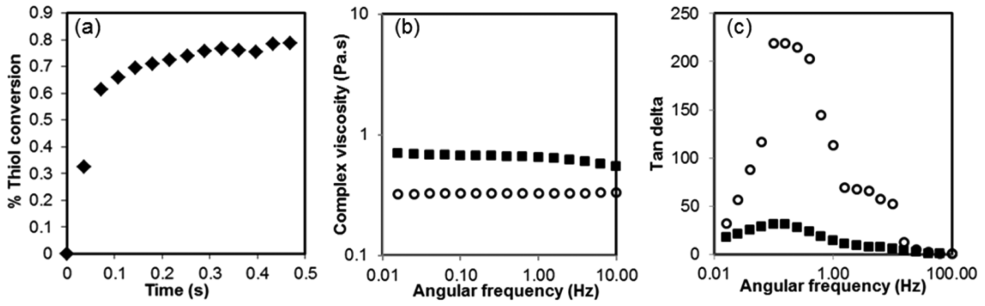

Figure 1. (a) Percent conversion of thiol groups upon exposure to UV light, as measured by IR spectroscopy. The fibers are 80% cured in 0.4 s and reach the gel point in 0.05 s. (b) Complex viscosity and (c) loss tangent as a function of oscillation frequency for a PETT/TVE mixture (open circles) and a PETT/TVE mixture with 0.6 wt % PMMA (solid squares).

3H), 4.37 (m, 6H), 4.16 (m, 3H), 3.98 (m, 3H), 3.73 (m, 6H), 1.83 (m, 12H).

Rheology. Small amplitude oscillatory shear experiments were performed using an AR 2000ex rheometer (TA Instruments) to determine the viscoelastic properties of the thiol−ene mixture with and without the addition of PMMA. A 40 mm diameter parallel plate assembly was used. To avoid curing issues in ambient light, photoinitiator was not added and the thiol−ene mixtures were immediately transferred to the rheometer plate as soon as they were prepared. Dynamic frequency sweep tests were performed at 25 °C over five decades of frequency (0.01 to 100 Hz), while maintaining the sample in its linear viscoelastic region.

Electrospinning Apparatus. The electrospinning apparatus consists of a high voltage DC supply (Gamma High Voltage Research ES40P, Florida), a syringe pump (Chemyx Fusion 200), and a grounded copper plate as a collector. The collector and needle tip were encased in ultraviolet-blocking Plexiglas to protect the user from harmful radiation. Light for curing was produced by a Scopelite 200 (Optical Building Blocks) metal halide lamp that produces light in the spectrum of 350−700 nm. A collimating lens was used to focus the light on the liquid jet while electrospinning fibers.

Electrospinning. The electrospinning solution was prepared by first dissolving 0.6 wt % PMMA into trivinyl ether at 70 °C for 18 h. After cooling this solution, PETT was mixed into it (corresponding to a 1:1 *thiol:ene* molar ratio); all PETT/TVE fibers/films in this study were made at this composition. To this mixture, 6 wt % of Igracure 2100 was added as photoinitiator, and the solution was mixed for 5 min at low speed to prevent bubble formation. The prepared solution was loaded into a syringe masked with black tape to block light exposure during spinning. All these steps were carried out in an environment that minimized UV light. The syringe was fitted with a 24-gauge blunt-tip needle with an inner diameter of 0.311 mm. The positive lead was attached to the tip of the needle, and the ground was attached to the copper plate positioned 16 cm from the tip of the needle. The solution was fed through the syringe at 1 mL/h. A 20 kV potential was applied once solution was visible at the end of the needle, creating a fluid jet. At this time, the light source was activated to cure the monomer fluid jet. The light was positioned about 10 cm from the fiber, and care was taken to point the light away from the needle tip and toward the collector, as described previously.[14] The light intensity at this distance was measured to be about 200 mW/cm^2.

Fourier Transform Infrared Spectroscopy (FTIR). A Nicolet 6700 FTIR spectrometer with a KBr beam splitter and MCT/A detector was used in rapid scan mode to investigate the curing kinetics of the solution. A drop of the prepared monomer mixture with photoinitiator was placed on a NaCl crystal and spread into a thin film by spin coating. The thickness of the film was targeted specifically to closely match the diameter of an average fiber made in this study. Sample preparations were performed in a room with no stray UV light and then loaded into the FTIR chamber equipped with a horizontal transmission accessory. The sample was continuously purged with zero grade air and a series scan was taken with 1 scan per spectrum resulting in spectra every 0.04 s. The scans were taken at ambient conditions at ∼25 °C. The monomer film was allowed to rest inside the FTIR with no light for approximately 2 min, at which point the light source was activated. The same light source with collimating lens was used at the same distance as used in fiber electrospinning. Data was collected until no more change in the IR spectra was detected. Thiol conversion was calculated by

$$\text{percent conversion} = 100 \times (A_0 - A_t)/A_0$$

Where A_0 is the area of the thiol peak (2570 cm^{-1}) before light exposure and A_t is the area of the thiol peak at a time after light exposure. All peak areas were normalized by a peak that is unchanged through the reaction.

Scanning Electron Microscopy (SEM). Fiber diameter was determined by a Hitachi S-4500 SEM. Fiber samples were placed on carbon tape and sputter-coated using an Au/Pd target. Images were taken with an accelerating voltage of 15 kV at a working distance of 15 mm. The images were analyzed by ImageJ software. Fiber diameter distribution was determined by measuring approximately 100 fibers on 20 different images.

Tensile Testing. The mechanical properties of single fibers and nonwoven mats were determined using a dynamic mechanical analyzer (DMA) (TA Instruments Q800). For nonwoven mats, samples of approximately 20 mm × 3 mm were cut from collected fiber mats and placed directly into the DMA grips. For obtaining single fibers, instead of collecting a well condensed mat we obtained a single layer deposition and carefully removed the individual fibers between the junction points in the fiber mat. Later, we used two parallel plates as collector and the fibers deposited between the plates were used for single fiber testing. We then prepared mounting "windows" for these fibers by cutting 3 cm × 3 cm squares of card stock. The fibers were mounted across the 1 cm^2 windows with tape. The taped ends were placed into the grips of the DMA tensile clamp, and the cardstock on the sides of the windows was cut, leaving only the fiber between the grips. Single fiber stress−strain tests were conducted using the DMA strain-rate mode at 5% and 60% strain per minute. Stress−strain tests on fiber mats were conducted at 60% strain per minute. Stretch-release cycling tests were also performed on the mats ramping stress at 0.3 MPa/min minute until 30% strain was reached and then the stress was removed at the same rate. All the tests were performed at 25 °C with 0.01 N preload force and 100 μm initial displacement. To determine the rubbery plateau modulus of the fibers, dynamic mechanical analysis was conducted on the fiber samples by ramping the temperature from −30 to 30 °C at a rate of 2 °C/min. These tests were conducted at a single frequency of 1 Hz and strain amplitude of 15 μm.

Differential Scanning Calorimetry. DSC scans were performed using a Mettler Toledo DSC1 to determine the glass transition temperature of PETT/TVE fibers. Multiple heating scans were performed from −60 to 150 °C at a heating rate of 10 °C/min.

Chemical Stability of the Fibers. The chemical stability of the fibers was evaluated by submerging the fibers in toluene or tetrahydrofuran at 60 °C for 4 h. The fibers were inspected by SEM before and after solvent exposure.

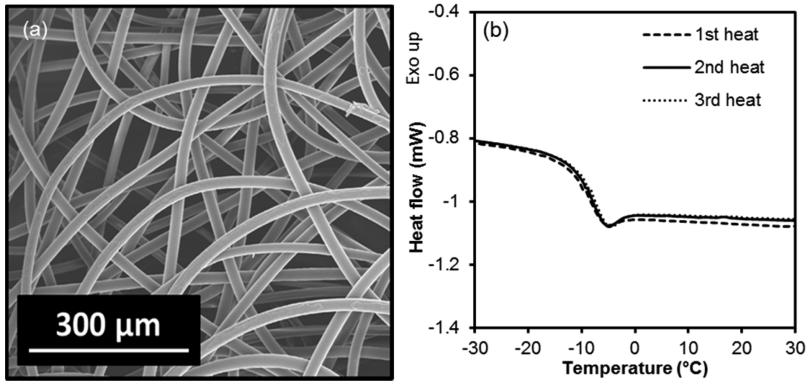

Figure 2. Representative (a) SEM image and (b) DSC thermogram of electrospun fibers from a PETT/TVE mixture along with 0.6 wt % PMMA and a photoinitiator.

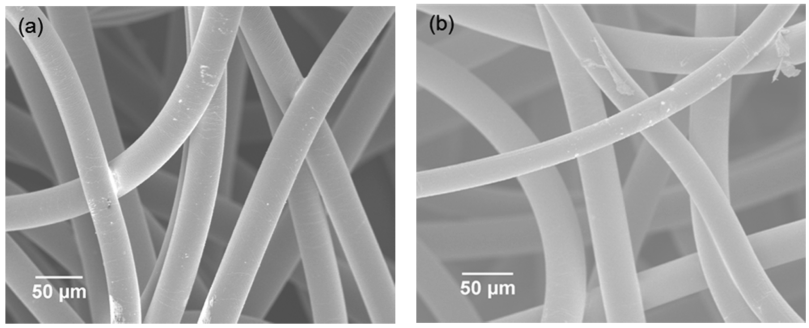

Figure 3. Representative SEM image of PETT/TVE fibers after submersion in (a) tetrahydrofuran and (b) toluene at 60 °C for 4 h.

RESULTS AND DISCUSSION

Single step conversion of small monomeric precursor molecules into highly elastic thermoset fibers by integrating thiol−ene photopolymerization and the electrospinning process requires careful consideration of curing kinetics and viscoelasticity of the spinning fluid. Considering the high velocity of the fluid jet during electrospinning (~1 m/s on average) and the available time (~0.2 s) for photopolymerizing the thiol−ene jet in situ, a very high speed curing system is necessary for producing defect-free fibers. Real time IR studies on thin films casted from a mixture of PETT/TVE along with 6 wt % photoinitiator and exposed to simulated light exposure conditions revealed that 80% of thiol groups are consumed in about 0.5 s (Figure 1a). With an equimolar mixture of thiol and vinyl reactive groups such as that examined in this study, the gel point α for an ideal step-growth polymerization of vinyl ether and thiols can be calculated using[15]

$$\alpha = [1/(f_{\text{thiol}} - 1)(f_{\text{ene}} - 1)]^{1/2}$$

where f_{thiol} and f_{ene} are the thiol and vinyl functionality, respectively. From this equation, the gelation is estimated to occur when 41% of thiol groups have reacted, which happens at about 0.05 s. So the curing speed is fast enough to produce a gelled fiber before the monomer mixture hits the collector for our fiber spinning conditions.

Viscoelastic properties of the spinning fluid also play a critical role on the spinnability of the monomer mixture. While low viscosity spinning solutions can result in droplet formation or a "beads on a string" morphology as surface tension subdues viscous forces, high viscosity solutions typically result in larger diameter fibers. It has also been shown that higher elasticity results in a lower variation in fiber diameter in melt-blown fiber systems.[21] Rheology experiments indicated that the complex viscosity of PETT and TVE in the Newtonian regime is about 0.33 Pa.s which is not adequate for electrospinning. In order to inhibit droplet formation and ensure defect-free fibers, the viscoelasticity of the thiol−ene mixture was enhanced by the addition of 0.6 wt % high-molecular weight (M_w = 1.5 × 10^6 g/mol) PMMA. Since PMMA has good solubility in vinyl ether and very high molecular weight versions of PMMA are commercially available, we chose to use it as an elasticity modifier. Apart from the increase in viscosity to about 0.65 Pa.s (Figure 1b), PMMA significantly increased the elasticity of the thiol−ene mixture, which can be confirmed by the drastic reduction in the loss tangent peak at low frequencies (Figure 1c). Tan delta is the ratio of loss or viscous modulus (G'') to the storage or elastic modulus (G'). The tan delta values were significantly reduced by the addition of PMMA to the monomer mixture owing to the increase in elastic modulus. This helped augment the viscoelastic behavior to enable electrospinning of PETT and TVE with 0.6 wt % PMMA and 6 wt % photoinitiator into high quality fibers.

A representative SEM micrograph of the fiber mat is shown in Figure 2. The fibers were smooth and solid with diameters ranging from 10 to 24 μm and an average diameter of about 20 μm. The fiber diameter can be further tuned by adjusting many parameters such as needle gauge, feed rate, electric field strength, etc. While the fibers produced in this work were mostly cured before deposition on the collector, additional reactions occur between some unreacted functional groups present on the surface of overlapping fibers, resulting in fused junctions. This yielded an extremely stable and robust nonwoven mat in one step without need for additional post treatments or binders.

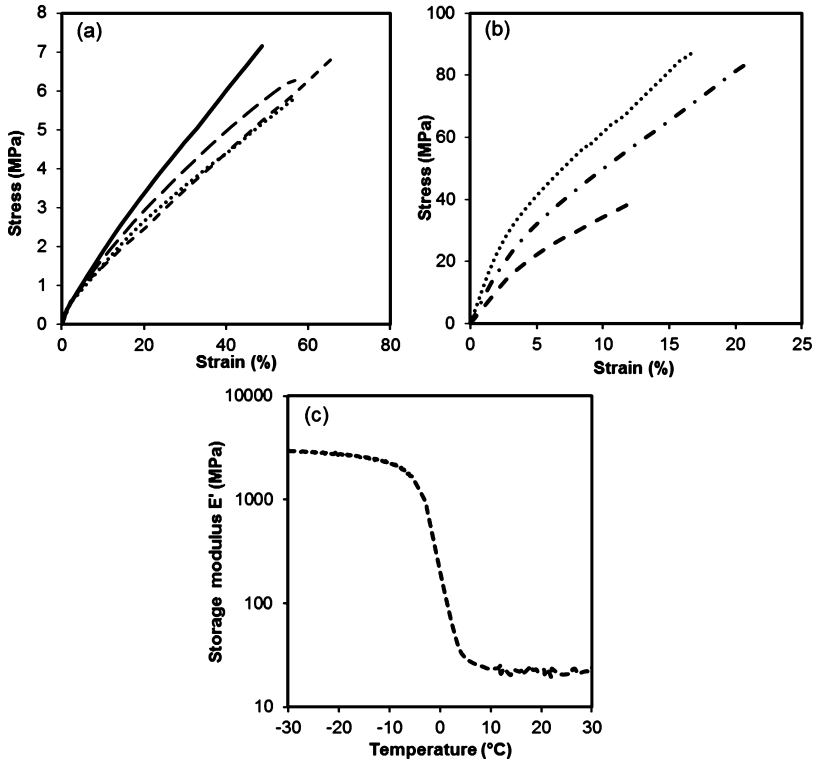

Figure 4. Stress/strain behavior of thiol−ene single fibers: (a) PETT/TVE fibers tested at 20 °C and 5% strain/min (dash and dotted lines from 3 individual tests) and 60% strain/min (solid line). (b) Pentaacrylate-based fibers made from 1:4.4 ratio of thiol to ene groups, tested at 130 °C and 5% strain/min (dash and dotted lines from 3 individual tests). Five to seven samples were tested for both PETT/TVE and pentaacrylate-based fibers and representative stress−strain traces are provided here for clarity. (c) Storage modulus as a function of temperature of PETT/TVE fibers tested at 1 Hz.

DSC thermograms on PETT/TVE fibers revealed a glass transition temperature (T_g) of about −9 °C (Figure 2b). A narrow and distinct glass transition was observed indicating a homogeneous cross-linked network, which is a typical characteristic of stoichiometric step-growth thiol−ene polymerizations. The fact that the T_g did not change significantly in successive DSC heat scans suggests that the fibers do not undergo significant post-thermal curing. Owing to the thermoset nature of these fibers, they exhibit very good chemical stability. The fibers remain smooth and unaffected in morphology or size even after exposing to tetrahydrofuran or toluene for 4 h at 60 °C. (Figure 3).

Figure 4 shows stress−strain data collected on single fibers. The fibers had an average elongation at break of 62% (sample size n = 5, standard deviation σ = 12.2), and average tensile strength of 6.6 MPa (n = 5, σ = 0.5), when subjected to tensile strain at two different strain rates viz, 5% strain/min and also a higher rate of 60% strain/min that is typically used for materials with higher elongation. It is remarkable that even at a higher strain rate the fibers had a high elongation at break of about 45% (solid line in in Figure 4a) close to 55−80% obtained at low strain rates (dash and dotted lines in Figure 4a). These fibers were very elastomeric compared to the pentaacrylate-based fibers in our previous work,[14] which had an elongation at break of only 8−13% at ambient temperature. DSC thermograms on PETT/TVE fibers revealed a glass transition temperature (T_g) of −9 °C, while the T_g of pentafunctional acrylate-based fibers was about 90 °C.[14] The elastomeric nature of vinyl ether fibers could be due to their lower T_g, since elastomers are typically lightly cross-linked amorphous polymers with a T_g below ambient temperature. However, stress strain tests (Figure 4b) conducted on pentafunctional acrylate-based fibers at 130 °C (i.e., well above their T_g) revealed an average elongation at break of only about 19% (n = 5, σ = 4.7). Although this is slightly higher than what is obtained at ambient conditions, the values are still much lower compared to vinyl ether based fibers. This suggests that the significant contrast in mechanical behavior of PETT/TVE fibers as compared to pentaacrylate-based fibers is not just a consequence of their subambient T_g, but also due to other factors such as differences in cross-link density, network homogeneity and monomer structure. The rubbery plateau modulus (E_r), which is proportional to cross-link density, is ∼10 MPa for PETT/TVE fibers (Figure 4c) and ∼10^3 MPa for pentaacrylate-based fibers.[14] Such a significant difference in the cross-link density can be expected from the higher functionality and relatively compact monomer structure of pentaacrylate (DPPA) as compared to the vinyl ethers used in this investigation (Scheme 1). This highlights the versatility of thiol−ene chemistry and how it can be favorably used to tune the mechanical properties of this new class of thermoset fibers.

While PETT/TVE fibers deform elastically without yielding until failure (Figure 4a), PETT/DPPA fibers show a decrease in modulus after 2.5% strain (Figure 4b). This strain hardening could be attributed to some irreversible deformation occurring at higher stress levels in the case of PETT/DPPA fibers. In addition, PETT/TVE fibers have a high polymer network homogeneity characteristic of step-growth thiol−ene systems.[22] Since the gel point of such networks occurs at high conversions, there is less stress built into the resulting polymer.[15] This results in high network homogeneity-meaning that there is little variation in the molecular weight between cross-links

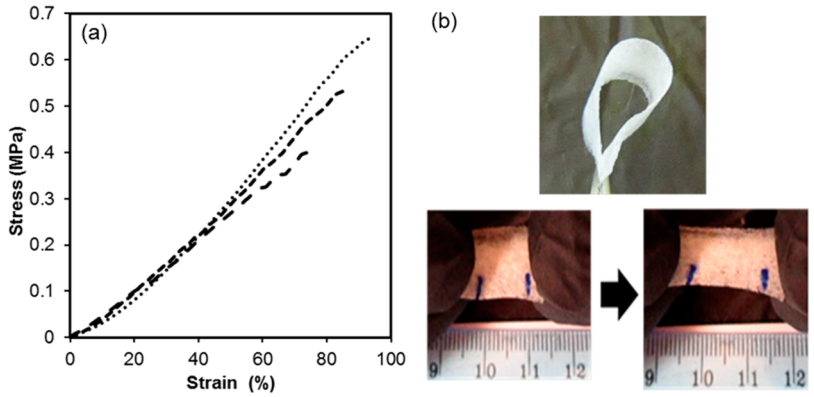

Figure 5. (a) Stress/strain behavior of nonwoven mats of PETT/TVE fibers tested at 20 °C and 60% strain/min (dash and dotted lines). Five samples were tested and 3 representative stress−strain traces are provided here for clarity. (b) Digital images of PETT/TVE nonwoven mat showing its flexible and stretchable nature.

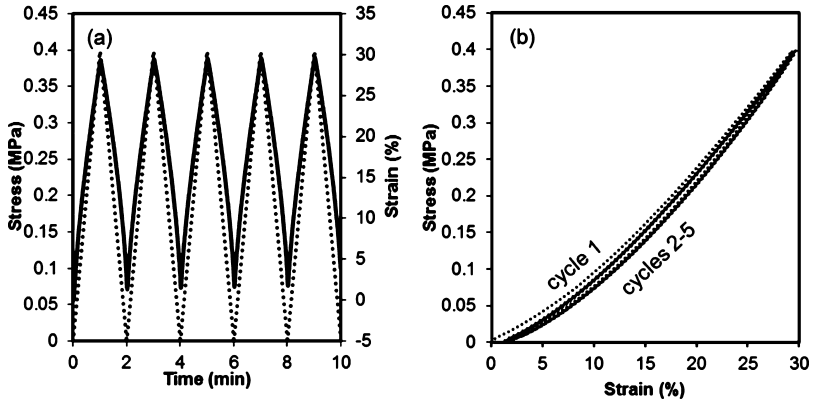

Figure 6. (a) Stress/strain cycling behavior (at 20 °C) of nonwoven mats of PETT/TVE fibers. The fiber mat shows 85−90% recovery of elongation as it is cycled from 0% strain to 30% strain over five cycles: stress (dotted line), strain % (solid line). (b) Data from part a replotted to reflect the hysteresis in stress/strain cycling.

throughout the polymer. This is in contrast to thiol−acrylate (PETT/DPPA) networks in which the acrylate homopolymer reacts rapidly, introducing stress into the network and lowering network homogeneity. The staged deformation phenomenon observed in the thiol−acrylate system could be attributed to this heterogeneous network, where higher stress levels can induce irreversible deformation in some portion of the network while other parts of the network prevent significant flow. Such phenomena have been observed in double network gels consisting of rigid and soft networks.[23]

An additional advantage of this fiber manufacturing approach is that the electrospun fibrous mats are mechanically robust to handle without additional post-treatments that are typically employed in the production of nonwoven mats. Although the liquid monomer jet photopolymerizes into solid fibers within a fraction of a second and most of the curing occurs in flight, we observed that some unreacted monomers present on the surface of the fibers in the overlapping regions react after deposition, resulting in fused junctions. It is worth noting that this feature could be easily controlled by changing the processing conditions. The fused junctions result in a mechanically robust mat that can be easily removed from the grounded collector and handled directly. Thus, the process is a one-step conversion of small monomeric molecules into mechanically robust three-dimensional nonwoven fibrous mats. Figure 5 shows the stress−strain behavior of nonwoven mats of PETT/TVE fibers. The mats were subjected to tensile strain at 60% strain/min at ambient conditions. Porous mats comprised of a three-dimensional network of PETT/TVE fibers showed significantly higher stretchability than the single fibers with an average elongation at break of about 85% (n = 5, σ = 6.2). During deposition, the photopolymerized fiber adopts curved and looped configurations between junction points, which can explain the higher stretchability of mats as compared to single fibers (Figure 4). When subjected to tensile forces, the fibers first straighten and align in the direction of the tensile force and then elongate until they break. This results in a lower slope (low modulus) at small strains with increasing modulus at higher strains. The number density of fibers in the mat and how they stretch, bend and align under uniaxial tensile loading governs the uniaxial tensile behavior of mats and this has been validated by micromechanical models.[24] Since the lay down of fibers and porosity are difficult to control in this fiber collection set up, the effect of porosity of the mat on stretchability could not be evaluated. Nonetheless the mats had an average tensile strength of about 0.6 MPa (n = 5, σ = 0.16). But precise estimation of tensile strength is difficult in such nonwoven fibrous mats as compared to single fibers or films owing to the porous and soft nature of the mat and the difficulty in accurate measurement of the thickness.

To test the robustness of the final polymer mat, we performed a strain cycling experiment wherein the fibrous mats were subjected up to about 30% strain and then released and this cycle was repeated 4−5 times. As shown in Figure 6a,

the mats showed significant elastic recovery of about 90−95% after the first cycle and 85−90% after the fifth cycle. There is some hysteresis (Figure 6b) associated with each stretch−release cycle. However, the area within the hysteresis loop becomes smaller after the first cycle and remains stable during successive cycles.

CONCLUSIONS

In summary, we have demonstrated a new approach for the production of stretchable thermoset fibers using the chemistry of thiol−ene photopolymerization. The method of production is not only simple but environmentally benign since it uses only non-volatile monomers as starting materials. PETT/TVE based single fibers have a high average elongation at break of 62% with good chemical and thermal stability. Mechanically robust nonwoven mats of PETT/TVE fibers can also be manufactured using this process without additional post-treatments and these mats have an average elongation at break of about 85%. Strain cycling experiments revealed that these mats can be stretched up to 30% with 85−90% elastic recovery after five cycles. Though we have used electrospinning in this investigation, recent work in our lab has shown that this green fiber manufacturing approach can be easily adapted to high throughput centrifugal Forcespinning, highlighting the broader scope and commercial viability of thiol−ene based thermoset fibers.

AUTHOR INFORMATION

Corresponding Author

*E-mail: ellison@che.utexas.edu.

Notes

The authors declare no competing financial interest.

ACKNOWLEDGMENTS

The authors wish to acknowledge Dr. Benny Freeman and Dr. Grant Willson for allowing use of their DMA and SEM facilities, respectively. This work was facilitated by partial financial support from the Welch Foundation (grant F-1709), DuPont Young Professor Award, and 3M Nontenured Faculty Award.

REFERENCES

(1) Gibson, P.; Schreuder-Gibson, H.; Rivin, D. Transport Properties of Porous Membranes Based on Electrospun Nanofibers. *Colloids Surf., A* **2001**, *187−188*, 469−481.

(2) Tan, A. R.; Ifkovits, J. L.; Baker, B. M.; Brey, D. M.; Mauck, R. L.; Burdick, J. A. Electrospinning of Photocrosslinked and Degradable Fibrous Scaffolds. *J. Biomed. Mater. Res., Part A* **2008**, *87A*, 1034−1043.

(3) Nair, D. P.; Cramer, N. B.; Scott, T. F.; Bowman, C. N.; Shandas, R. Photopolymerized Thiol-Ene Systems as Shape Memory Polymers. *Polymer* **2010**, *51*, 4383−4389.

(4) Peñalver, E.; Grimaldi, D. A.; Delclòs, X. Early Cretaceous Spider Web with Its Prey. *Science* **2006**, *312*, 1761.

(5) Gosline, J. M.; DeMont, M. E.; Denny, M. W. The Structure and Properties of Spider Silk. *Endeavour* **1986**, *10*, 37−43.

(6) Scheller, J.; Conrad, U. Plant-Based Material, Protein and Biodegradable Plastic. *Curr. Opin. Plant Biol.* **2005**, *8*, 188−196.

(7) Xia, X.-X.; Qian, Z.-G.; Ki, C. S.; Park, Y. H.; Kaplan, D. L.; Lee, S. Y. Native-sized Recombinant Spider Silk Protein Produced in Metabolically Engineered Escherichia Coli Results in a Strong Fiber. *Proc. Natl. Acad. Sci. U.S.A.* **2010**, *107*, 14059−14063.

(8) Lazaris, A.; Arcidiacono, S.; Huang, Y.; Zhou, J.-F.; Duguay, F.; Chretien, N.; Welsh, E. A.; Soares, J. W.; Karatzas, C. N. Spider Silk Fibers Spun from Soluble Recombinant Silk Produced in Mammalian Cells. *Science* **2002**, *295*, 472−476.

(9) Broise A. R. Manufacture of Rubber Threads. US Patent 2,333,699, 1943.

(10) Miller, J. A., Jr; Nagarajan, V. The Impact of Biotechnology on The Chemical Industry in the 21st Century. *Trends Biotechnol.* **2000**, *18*, 190−191.

(11) Warner, S. B. *Fiber Science*, 1st ed; Prentice Hall Publications: Englewood Cliffs, NJ, 1995.

(12) Liu, L.; Zhang, F.; Hu, S.; Zhang, L.; Wen, S. Preparation of Ultrafine Ethylene/Propylene/Diene Terpolymer Rubber Fibers by Coaxial Electrospinning. *Macromol. Mater. Eng.* **2012**, *297*, 298−302.

(13) Kim, S. H.; Kim, S.-H.; Nair, S.; Moore, E. Reactive Electrospinning of Cross-Linked Poly(2-hydroxyethyl methacrylate) Nanofibers and Elastic Properties of Individual Hydrogel Nanofibers in Aqueous Solutions. *Macromolecules* **2005**, *38*, 3719−3723.

(14) Shanmuganathan, K.; Sankhagowit, R. K.; Iyer, P.; Ellison, C. J. Thiol−Ene Chemistry: A Greener Approach to Making Chemically and Thermally Stable Fibers. *Chem. Mater.* **2011**, *23*, 4726−4732.

(15) Hoyle, C. E.; Lee, T. Y.; Roper, T. Thiol-enes: Chemistry of the Past with Promise for the Future. *J. Polym. Sci., Part A: Polym. Chem.* **2004**, *42*, 5301−5338.

(16) Hoyle, C. E.; Bowman, C. N. Thiol-Ene Click Chemistry. *Angew. Chem., Int. Ed.* **2010**, *49*, 1540−1573.

(17) Kwisnek, L.; Nazarenko, S.; Hoyle, C. E. Oxygen Transport Properties of Thiol-Ene Networks. *Macromolecules* **2009**, *42*, 7031−7041.

(18) Walker, C. N.; Versek, C.; Touminen, M.; Tew, G. N. Tunable Networks from Thiolene Chemistry for Lithium Ion Conduction. *ACS Macro Lett.* **2012**, *1*, 737−741.

(19) Cramer, N. B.; Bowman, C. N. Kinetics of Thiol−ene and Thiol−acrylate Photopolymerizations with Real-time Fourier Transform Infrared. *J. Polym. Sci., Part A: Polym. Chem.* **2001**, *39*, 3311−3319.

(20) Cramer, N. B.; Scott, J. P.; Bowman, C. N. Photopolymerizations of Thiol-ene Polymers without Photoinitiators. *Macromolecules* **2002**, *35*, 5361−5365.

(21) Tan, D. H.; Zhou, C. F.; Ellison, C. J.; Kumar, S.; Macosko, C. W.; Bates, F. S. Meltblown Fibers: Influence of Viscosity and Elasticity on Diameter Distribution. *J. Non-Newton. Fluid Mech.* **2010**, *165*, 892−900.

(22) Senyurt, A. F.; Wei, H.; Hoyle, C. E.; Piland, S. G.; Gould, T. E. Ternary Thiol−Ene/Acrylate Photopolymers: Effect of Acrylate Structure on Mechanical Properties. *Macromolecules* **2007**, *40*, 4901−4909.

(23) Haque, M. A.; Kurokawa, T.; Kamita, G.; Gong, J. P. Lamellar Bilayers as Reversible Sacrificial Bonds To Toughen Hydrogel: Hysteresis, Self-Recovery, Fatigue Resistance, and Crack Blunting. *Macromolecules* **2011**, *44*, 8916−8924.

(24) Silberstein, M. N.; Pai, C.-L.; Rutledge, G. C.; Boyce, M. C. Elastic−plastic Behavior of Non-woven Fibrous Mats. *J. Mech. Phys. Solids* **2012**, *60*, 295−318.